Controllable powers range and control method of DFIG for transient stability of power system

Di Zheng, Jinxin Ouyang, Xiaofu Xiong

State Key Laboratory of Power Transmission Equipment & System Security and New Technology, Chongqing University, Chongqing 400044, People's Republic of China
E-mail: di.zh@foxmail.com

Published in *The Journal of Engineering*; Received on 10th October 2017; Accepted on 2nd November 2017

Abstract: Wind generation is increasing rapidly in the grid, which has greater impacts on the power system than ever. The impacts are more serious under grid fault. The low-voltage ride through (LVRT) controls of doubly fed induction generators (DFIGs) may change characteristics of synchronous generators (SGs) and threaten the transient stability of power system. However, the influence on the transient stability and even the controllable powers of a DFIG has not been considered in the existing LVRT method. The contributions of the reactive power supplied by a DFIG in the oscillation process of power angle of SG were analysed. The controllable range of powers of a DFIG was researched with consideration of the rotor speed limit. An LVRT control method of a DFIG based on the controllable range was proposed to improve the transient stability of power system. Simulations show that the proposed method could enhance the power angle stability of power system under the condition of avoiding overspeed and out of service of DFIG.

1 Introduction

Driven by fossil energy depletion and renewable energy demand, the doubly fed induction generators (DFIGs) have developed rapidly and become mainstream generators for power systems [1]. With the increase in wind power installed capacity, the DFIG is required to keep connecting to the grid in the fault and provide reactive power to support the recovery of grid voltage [2].

The DFIG output reactive power in the low-voltage ride through (LVRT) process in accordance with the reactive current reference, while will increase terminal voltage of synchronous generator (SG) in the grid and have impact on its power angle stability [3–5]. It is pointed out in [6] that the DFIG participates in oscillation process of SG's power angle as a power source, which means a lack of inertia. Transient output of the DFIG is treated as a negative impendence and researched on the impact of the DFIG's active power control strategy and reactive power control strategy on the power angle characteristics in [7]. However, transient characteristics of DFIG depend on control modes and parameters. The impact of the DFIG on power angle characteristics of the SG has not represented clearly and deeply in existing researches. Activating LVRT control immediately after the grid fault is the main means to realise fault riding through of wind turbines. At present, the related researches on LVRT control mainly focus attaching hardware and control structure improvement to meet the wind farm LVRT standard. However, the LVRT standard aims to support the grid voltage. The existing LVRT control methods did not consider the impacts of DFIG's output during LVRT process on transient stability of the grid.

The effect of a DFIG during the LVRT process on the grid depends mainly on its reactive power capacity. At present, the reactive power capacity of a DFIG has been studied while related researches focused on the converter current limit [8–10]. Active power of the DFIG during LVRT process effects reactive power limit indirectly [8]. The turbine of a DFIG needs to regulate the pitch angle to reduce mechanical power for avoiding operation of overspeed protection and the generator shutdown [11, 12]. The rate of pitch angle regulating is limited by the mechanical actuator, which is much slower than the change of electromagnetic power. Excessive reactive power means insufficient active power, which is unable to balance the slower mechanical power. It will lead to excessive acceleration of the rotor and overspeed protection will cut the generator off the grid.

In general, this paper analysed the impact of the DFIG on SG's power angle. Controllable power range of the DFIG was studied for SG's power angle stability improvement. Finally, an LVRT method based on controllable power range of the DFIG to improve SG's power angle stability was proposed.

2 Transient process of DFIG

The stator of a DFIG is connected directly to the grid while the rotor is connected through a back-to-back converter, of which control system keeps output power steady. The math model of a DFIG is usually composed of stator's and rotor's voltage equations and flux linkage equations as follows:

$$\begin{cases} \boldsymbol{u}_{\mathrm{Ds}} = R_{\mathrm{Ds}}\boldsymbol{i}_{\mathrm{Ds}} + \mathrm{j}\omega_{\mathrm{s}}\boldsymbol{\psi}_{\mathrm{Ds}} + \mathrm{d}\boldsymbol{\psi}_{\mathrm{Ds}}/\mathrm{d}t \\ \boldsymbol{u}_{\mathrm{Dr}} = R_{\mathrm{Dr}}\boldsymbol{i}_{\mathrm{Dr}} + \mathrm{j}\omega_{p}\boldsymbol{\psi}_{\mathrm{Dr}} + \mathrm{d}\boldsymbol{\psi}_{\mathrm{Dr}}/\mathrm{d}t \\ \boldsymbol{\psi}_{\mathrm{Ds}} = L_{\mathrm{Ds}}\boldsymbol{i}_{\mathrm{Ds}} + L_{\mathrm{Dm}}\boldsymbol{i}_{\mathrm{Dr}} \\ \boldsymbol{\psi}_{\mathrm{Dr}} = L_{\mathrm{Dr}}\boldsymbol{i}_{\mathrm{Dr}} + L_{\mathrm{Dm}}\boldsymbol{i}_{\mathrm{Ds}} \end{cases} \tag{1}$$

in which $\boldsymbol{u}$, $\boldsymbol{i}$ and $\boldsymbol{\psi}$ are, respectively, voltage vector, current vector and flux linkage vector.

We can ignore the resistances of the stator and rotor due to their small values. So that transient stator flux linkage in fault steady state can be expressed as

$$\boldsymbol{\psi}_{\mathrm{Ds}} = \frac{\boldsymbol{u}_{\mathrm{Ds}}}{\mathrm{j}\omega_{\mathrm{s}}} \tag{2}$$

The LVRT control is activated immediately after the grid fault occurs. The outer loop of rotor-side converter (RSC) of the DFIG

doi: 10.1049/joe.2017.0605

is locked and the current reference of inner loop is set up directly [13]. The reactive power of the DFIG can be adjusted by changing reactive current reference to support the grid voltage. Utilising the PI regulator, the control equation of RSC's inner loop is given by

$$\boldsymbol{u}_{\mathrm{Dr}}^{*}=k_{\mathrm{p}}\left(\boldsymbol{i}_{\mathrm{Dr}}^{*}-\boldsymbol{i}_{\mathrm{Dr}}\right)+k_{\mathrm{i}}\left(\boldsymbol{i}_{\mathrm{Dr}}^{*}-\boldsymbol{i}_{\mathrm{Dr}}\right)+\mathrm{j}\omega_{\mathrm{p}}\boldsymbol{i}_{\mathrm{Dr}} \tag{3}$$

where $\boldsymbol{u}_{\mathrm{Dr}}^{*}$, $\boldsymbol{i}_{\mathrm{Dr}}^{*}$ are the rotor voltage vector and the rotor current vector and k_{p}, k_{i} are the proportion coefficient and integral coefficient, respectively.

The inner loop of the RSC is usually designed as typical I system to realise fast track capacity. Thus, the transient duration is so short that it can be neglected in the analysis of electromechanical transient process [14], which means $\boldsymbol{i}_{\mathrm{Dr}}$ can track $\boldsymbol{i}_{\mathrm{Dr}}^{*}$ ideally. Substituting (2) into the flux linkage equations of the stator and rotor, the stator current is obtained as

$$\boldsymbol{i}_{\mathrm{Ds}}=\frac{\boldsymbol{u}_{\mathrm{Ds}}-\mathrm{j}x_{\mathrm{Dm}}\boldsymbol{i}_{\mathrm{Dr}}^{*}}{\mathrm{j}x_{\mathrm{Ds}}} \tag{4}$$

where x_{Dm} and x_{Ds} are the excitation reactance and stator reactance, respectively.

When the stator-flux-oriented vector control is employed in the RSC, the stator flux is aligned with the d-axis of the synchronous reference frame. Then the stator voltage is aligned with the q-axis according to (2). Based on the definition of instantaneous power, the stator powers are expressed as

$$\begin{cases} P_{\mathrm{Ds}}=-\mathrm{Re}\left[\boldsymbol{u}_{\mathrm{Ds}}\hat{\boldsymbol{i}}_{\mathrm{Ds}}\right]=\dfrac{x_{\mathrm{Dm}}}{x_{\mathrm{Ds}}}U_{\mathrm{Ds}}i_{\mathrm{Drq}}^{*} \\ Q_{\mathrm{Ds}}=-\mathrm{Im}\left[\boldsymbol{u}_{\mathrm{Ds}}\hat{\boldsymbol{i}}_{\mathrm{Ds}}\right]=\dfrac{x_{\mathrm{Dm}}U_{\mathrm{Ds}}i_{\mathrm{Drd}}^{*}-U_{\mathrm{Ds}}^{2}}{x_{\mathrm{Ds}}} \end{cases} \tag{5}$$

where i_{Drd}^{*} and i_{Drq}^{*} are the d-axis and q-axis components of the current reference of the RSC, respectively. U_{Ds} is the amplitude of the stator voltage vector.

3 Power angel characteristics machine system of double-machine system

A double-machine system consisting of a DFIG and an SG is shown in Fig. 1. When a metallic fault occurs at point f, an equivalent circuit of the system can be built as Fig. 2 in which $\boldsymbol{e}_{S0}=e_{S0}\angle\left(\phi+90^{\circ}\right)$ is the no-load electromotive force of the SG in the DFIG's synchronous reference frame. e_{S0} is the amplitude and ϕ is the angle between the q-axis of the SG′ synchronous

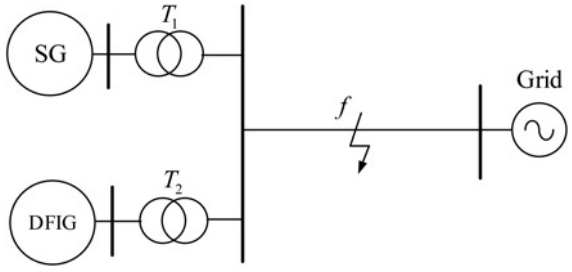

Fig. 1 *Structure of double-machine system*

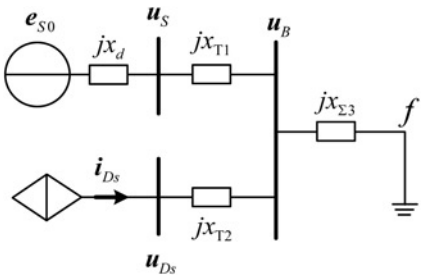

Fig. 2 *Equivalent circuit of double-machine system*

reference frame and that of the DFIG's synchronous reference frame. x_d is the synchronous reactance of the SG and x_{T1}, x_{T2} are the equivalent reactances of the SG's and DFIG's transformers, respectively. $x_{\Sigma 3}$ is the reactance from Bus B to point f. According to the equivalent circuit, the principles of currents and voltages are obtained as

$$\frac{\boldsymbol{e}_{S0}-\boldsymbol{u}_B}{\mathrm{j}x_{\sum 1}}+\boldsymbol{i}_{\mathrm{Ds}}=\frac{\boldsymbol{u}_B}{\mathrm{j}x_{\sum 3}} \tag{6}$$

$$\boldsymbol{u}_{Ds}-\boldsymbol{u}_B=\mathrm{j}x_{\mathrm{T2}}\boldsymbol{i}_{Ds} \tag{7}$$

where $x_{\sum 1}=x_d+x_{\mathrm{T1}}$.

Substituting (4) into (6) and (7), the Bus B voltage and the stator voltage of the DFIG are given by

$$\boldsymbol{u}_b=\frac{x_{\sum 3}(x_{T2}-x_s)}{\beta-\alpha x_s}\boldsymbol{e}_{S0}+\mathrm{j}\frac{x_m x_{\sum 1}x_{\sum 3}}{\beta-\alpha x_s}\boldsymbol{i}_{\mathrm{Dr}}^{*} \tag{8}$$

$$\boldsymbol{u}_{\mathrm{Ds}}=\frac{\mathrm{j}x_{\mathrm{Ds}}x_{\mathrm{m}}\beta}{\beta-\alpha x_{\mathrm{Ds}}}\boldsymbol{i}_{\mathrm{Dr}}^{*}-\frac{x_{\mathrm{Ds}}x_{\sum 3}}{\beta-\alpha x_{\mathrm{Ds}}}\boldsymbol{e}_{S0} \tag{9}$$

where $\alpha=x_{\sum 1}+x_{\sum 3}$ and $\beta=x_{\mathrm{T2}}x_{\sum 1}+x_{\sum 1}x_{\sum 3}+x_{\mathrm{T2}}x_{\sum 3}$.

$\boldsymbol{u}_{\mathrm{Ds}}$ is consisted by the q-axis component only, which means the real part in (9) is zero. Substituting this into (8), the amplitude of the Bus B voltage is obtained as (see (1))

where $\lambda=x_{\mathrm{Dm}}x_{\sum 1}$ and $\gamma=x_{\mathrm{Ds}}-x_{\mathrm{T2}}$.

Taking partial derivative of (10) to i_{Drd}^{*} and i_{Drq}^{*}, respectively, we get

$$\frac{\mathrm{d}u_B}{\mathrm{d}i_{\mathrm{Drd}}^{*}}<0,\quad \frac{\mathrm{d}u_B}{\mathrm{d}i_{\mathrm{Drq}}^{*}}>0 \tag{11}$$

which means amplitude of the Bus B voltage increases with i_{Drd}^{*} decreasing and increases with i_{Drq}^{*} increasing.

The power angle characteristic of the SG which is shown in Fig. 3 can be described as

$$P_{\mathrm{SG}}=\frac{e_{S0}x_{\sum 3}\sin\delta}{x_{\sum 1}(\beta-\alpha x_d)}\Big[\gamma^2e_{S0}^2+\lambda^2i_{\mathrm{Dr}}^{*2} -2\lambda x_m\beta\gamma\left(i_{\mathrm{Drq}}^{*2}-i_{\mathrm{Drd}}^{*}\sqrt{\frac{x_{\sum 3}^2}{x_m^2\beta^2}e_{S0}^2-i_{\mathrm{Drq}}^{*2}}\right)\Big]^{1/2} \tag{12}$$

$$u_B=\frac{x_{\sum 3}\sqrt{\gamma^2e_{S0}^2+\lambda^2i_{\mathrm{Dr}}^{*2}-2\lambda x_{\mathrm{Dm}}\beta\gamma\left(i_{\mathrm{Drq}}^{*2}-i_{\mathrm{Drd}}^{*}\sqrt{\dfrac{x_{\sum 3}^2}{x_{\mathrm{Dm}}^2\beta^2}e_{S0}^2-i_{\mathrm{Drq}}^{*2}}\right)}}{\beta-\alpha x_{\mathrm{Ds}}} \tag{10}$$

doi: 10.1049/joe.2017.0605

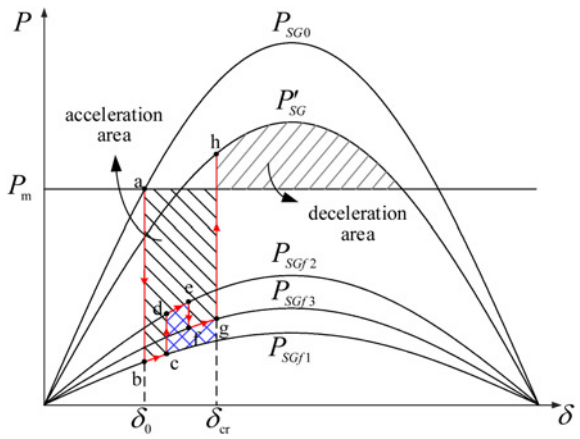

Fig. 3 *Power angle characteristic of SG with impact of DFIG*

where P_{SG} is the active power of the SG and S is the power angle. From (12), we know that by changing the reference of the RSC, the DFIG changes output power to influence amplitude of the stator voltage of the SG. So the power angle characteristic of the SG is still a sine wave and only amplitude of it is changed by the DFIGURE. Without considering the DFIG, the operation point of the SG moves from point a on P_{SG0} to point b on P_{SGf1} after the grid fault happens. Meanwhile the rotor of the SG accelerates since the active power is smaller than the mechanical power. We assume that the LVRT control activates at point c. Then the reactive power of the DFIG increases with i^*_{Drq} increasing which leads to larger stator voltage of the SG. The active power of the SG increases and the operation point moves from point c to point d. Then at point e i^*_{Drd} is set to be larger which means larger active power of the DFIG, lower stator voltage and smaller active power of the SG. The operation point moves from point e to point f. After the grid fault is cleared at point g, the operation point of the SG returns to point h on P'_{SG}. Comparing with the situation without the DFIG, the DFIG makes the accelerate area smaller by the crossline area. It is concluded that larger q-axis current reference of the RSC is more beneficial to the power angle stability of the SG while d-axis current reference is opposite.

4 Control method of the DFIG considering power controllable range

4.1 Controllable range of active power

During the LVRT process, the DFIG has to adjust the pitch angle to keep rotating speed of the generator in an acceptable range. However, too small active power may lead to pitch control not in time so that the rotor accelerates too fast, overspeed protection operates and the generator is shutdown. A reasonable active power is expected to avoid this situation:

$$\int_0^{t_{lst}} \left(P_{Dm} - P_{Ds}\right) \mathrm{d}t \le M\left(\omega_{Dr\,max} - \omega_{Dr0}\right) \tag{13}$$

where t_{lst} is the duration of the DFIG's LVRT control. P_{Dm} is the mechanical power of the turbine transmitted to the generator. M is the inertia constant of the DFIG generator's rotor. $\boldsymbol{\omega}_{Dr\ max}$ is the overspeed protection actuating value. $\boldsymbol{\omega}_{Dr0}$ is the initial rotating speed of the DFIG generator before the fault happens.

The mechanical power of the DFIG turbine is described as

$$P_{Dm} = P_w C_P \tag{14}$$

where $P_w = 0.5\rho\pi R^2 v_w^3$ is the wind power flowing through the swept area in which ρ is the air density, R is the radius of the DFIG turbine's blade and v_w is the wind speed. The wind power coefficient C_p is a function of the tip speed ratio λ and the pitch angle β. λ can be obtained as $\lambda = \omega_w R/v_w$ in which ω_w is the rotating speed of the DFIG turbine's blade. Utilising the numerical approximation method, C_p is expressed as [15, 16]

$$\begin{cases} \chi = \dfrac{1}{\lambda + 0.08\beta} - \dfrac{0.035}{\beta^3 + 1} \\ C_P = 0.22\left(116\chi - 0.4\beta - 5.0\right)\mathrm{e}^{-12.5\chi} \end{cases} \tag{15}$$

Due to the large inertia of the DFIG turbine, we assume λ remains the optional tip speed ratio during the pitch angle regulating process. When the rotating speed of the DFIG generator is not lager than the rating speed, the pitch angle is zero. The optional tip speed ratio can be calculated as $\lambda_{opt} = 6.345$ using (15). C_p is expressed as a function of β with using a numerical fitting method:

$$C_P = -0.0002856\beta(t)^2 - 0.01166\beta(t) + 0.4383 \tag{16}$$

The maximum pitch angle regulating speed during the emergency feathering is about 10°–20°/s [16]. We set the average regulating speed to be 10°/s and (16) can be transformed as

$$C_P = -0.02856t^2 - 0.1166t + 0.4383 \tag{17}$$

Substituting (14) and (17) into (13), the expected minimum active power $P_{Ds\ min}$ is obtained. If $\omega_{Dr0} \le \omega_{Dr\ max} - P_w f\left(t_{lst}\right)/M$, we get $P_{Ds\ min} = 0$. If $\omega_{Dr0} \le \omega_{Dr\ max} - P_w f\left(t_{lst}\right)/M$, $P_{Ds\ min}$ is calculated as

$$P_{Ds\ min} = \frac{P_w f(t_{lst}) - M(\omega_{Ds\ max} - \omega_{Dr0})}{t_{lst}} \tag{18}$$

where $f\left(t_{lst}\right) = -0.00952t_{lst}^3 - 0.0583t_{lst}^2 + 0.4383t_{lst}$.

It is hard to calculate t_{lst} for the uncertain fault duration. To keep the DFIG generator not overspeed in any certain situation, the maximum rotating speed of the DFIG generator should be smaller than $\omega_{Dr\ max}$ when the accelerated speed is zero, namely $P_{Dm} = P_{Ds\ min}$. So t_{lst} t is obtained as

$$t_p = \sqrt[3]{\sqrt{689.61\mu^2 + 55.84\mu} - 26.26\mu - 1.06} - 1.02 + \frac{1.04}{\sqrt[3]{\sqrt{689.61\mu^2 + 55.84\mu} - 26.26\mu - 1.06}} \tag{19}$$

where $\mu = M\omega_{DrN}^3\left(\omega_{Dr0} - \omega_{Dr\ max}\right)/\omega_{Dr0}^3$ and ω_{DrN} are the rating rotating speed of the DFIG generator.

Thus, the minimum active power of the DFIG can be described as follows:

(i) if $\omega_{Dr0} \le \omega_{Dr\,max} - P_w f(t_p)/M$, $P_{Ds\,min} = 0$;
(ii) if $\omega_{Dr0} \le \omega_{Dr\,max} - P_w f(t_p)/M$,

$$P_{Ds\ min} = \frac{P_w f(t_p) - M(\omega_{Dr\ max} - \omega_{Dr0})}{t_p} \tag{20}$$

4.2 Controllable range of reactive power

For the security of the converters, the rotor current should be no larger than the maximum allowable running current which means as

$$i^{*2}_{Drd} + i^{*2}_{Drq} \le i^2_{Dr\ max} \tag{21}$$

where $I_{Dr\ max}$ the maximum allowable running current of the RSC.

doi: 10.1049/joe.2017.0605

Combining (5) and (21), the reactive power of the DFIG is expressed as

$$Q_{\mathrm{Ds}} \le -\frac{u_{\mathrm{Ds}}^2}{x_{\mathrm{Ds}}} + \sqrt{\left(\frac{x_{\mathrm{Dm}}u_{\mathrm{Ds}}}{x_{\mathrm{Ds}}}\right)^2 I_{\mathrm{Dr\,max}}^2 - P_{\mathrm{Ds}}^2} \tag{22}$$

Substituting the active power expression into (22), the maximum reactive power under the constraints of the converter current and rotor rotating speed is described as

$$Q_{\mathrm{Ds\,max}} \le -\frac{u_{\mathrm{Ds}}^2}{x_{\mathrm{Ds}}} + \sqrt{\left(\frac{x_{\mathrm{Dm}}u_{\mathrm{Ds}}}{x_{\mathrm{Ds}}}\right)^2 I_{\mathrm{Dr\,max}}^2 - P_{\mathrm{Ds\,min}}^2} \tag{23}$$

The controllable power operation area of the DFIG is shown in Fig. 4. With the initial rotating speed of the DFIG generator decreasing, the area for the rotor accelerating is increasing which means smaller $P_{\mathrm{Ds\ min}}$, larger $Q_{\mathrm{Ds\ max}}$ and larger controllable power operation range. If the initial rotating speed is smaller than a certain value ω'_{Dr0}, $P_{\mathrm{Ds\ min}}$ turns to zero which means the DFIG generator's rotor will never overspeed whatever $Q_{\mathrm{Ds\ max}}$ is. $Q_{\mathrm{Ds\ max}}$ could reach the limit of the converter current. From (12), for the good of the SG's power angle stability and the DFIG's controllability, $P_{\mathrm{Ds\ min}}$ and $Q_{\mathrm{Ds\ max}}$ obtained above are what we want.

4.3 LVRT method of the DFIG

Based on the controllable range of the DFIG above, the control block of the DFIG's LVRT method is shown in Fig. 5. In the steady condition, double closed loop is used to control the active and reactive power in the RSC. The power loop provides the reference value for the current loop. The LVRT control and emergency feathering are activated immediately after the grid fault occurs. Firstly, we judge that the initial rotating speed ω_{Dr0} is in the active power limited area or not, namely, if ω_{Dr0} is smaller than ω'_{Dr0} or not. If ω_{Dr0} is smaller than ω'_{Dr0}, set $P_{\mathrm{Ds\ min}}$ to be zero. If ω_{Dr0} is larger than ω'_{Dr0}, set $P_{\mathrm{Ds\ min}}$ according to (20). Then we calculate $Q_{\mathrm{Ds\ max}}$ using (22). With $P_{\mathrm{Ds\ min}}$, $Q_{\mathrm{Ds\ max}}$ and the stator voltage of the DFIG U_{Ds}, i^*_{Drd} and i^*_{Drq} are calculated by (5). Finally, we lock the power loop of the RSC, switch the current reference from port 1 to port 2 and the LVRT control starts. The flowchart of the LVRT control method is shown in Fig. 6.

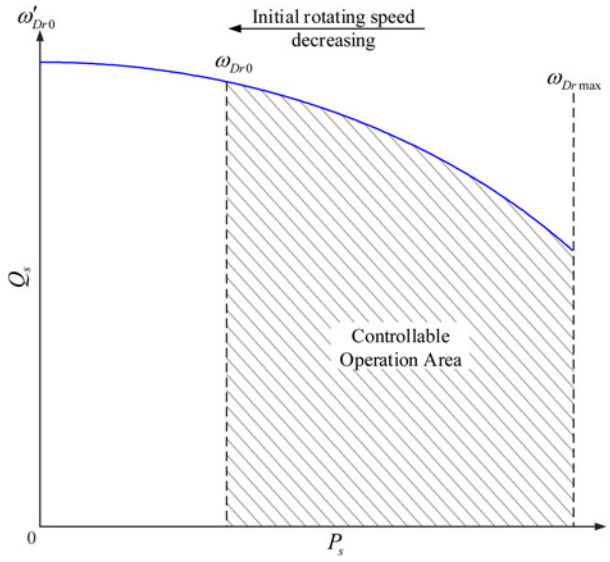

Fig. 4 *Powers controllable area of a DFIG*

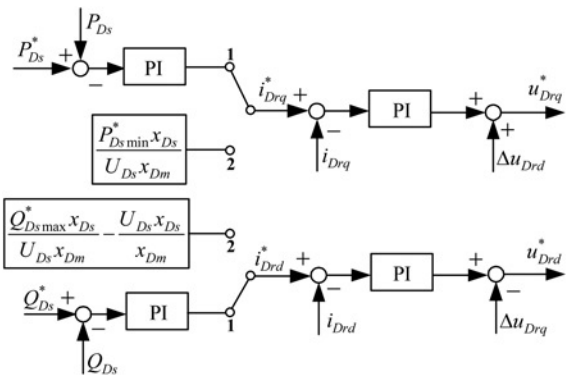

Fig. 5 *Control block of the LVRT method of the DFIG*

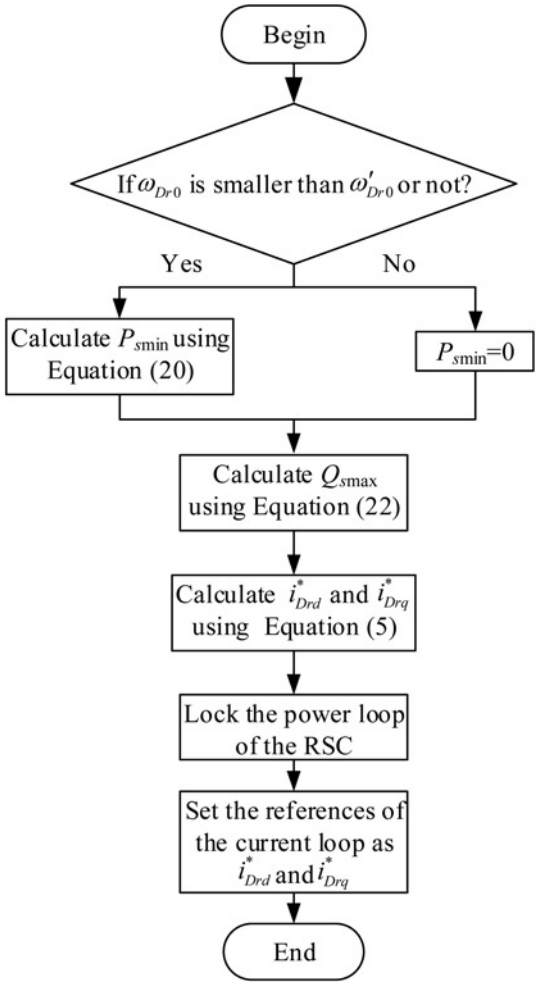

Fig. 6 *Flowchart of the LVRT control of DFIG*

5 Simulations

A simulation system shown in Fig. 7 is built in MATLAB/Simulink in which the DFIG and the SG connects to the grid through the same bus and a 100 km transmission line. The rating capacity of the SG is 300 MVA and the initial active power is 120 MW. The rating capacity, rating wind speed, rating rotating speed, overspeed protection actuating value and the maximum RSC current of the

doi: 10.1049/joe.2017.0605

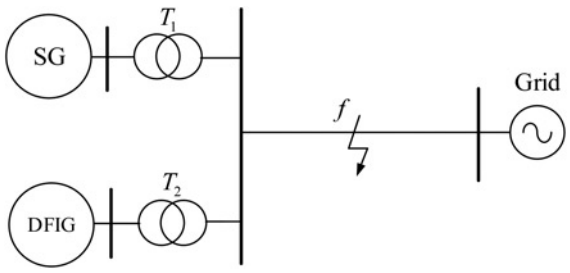

Fig. 7 *Simulation system of a double-machine system*

DFIG are, respectively, 225 MW, 15 m/s, 1.2, 1.3 and 1.1 p.u. The DFIG operates in the unit-power-factor mode in the steady condition. The LVRT control is activated immediately after the fault occurs which means the power loop of the RSC is locked and the reference of the current loop is set up directly. At the meanwhile the pitch angle is regulated by 10°/s.

The symmetric permanent fault occurs at point f when $t = 1$ s. 4 simulation conditions are set as in Table 1. In Cases 1 and 2, the stator voltage of the DFIG falls to 0.7 p.u., i^*_{Drq} is the same while i^*_{Drd} are different. In Cases 3 and 4, the wind speed is 15 m/s and the stator voltage of the DFIG falls to 0.28 p.u. In Case 3, i^*_{Drd} is set as 1.08 p.u. according to existing wind power connecting rules and i^*_{Drq} is set as 0.20 p.u. In Case 4, the DFIG uses the LVRT method proposed which means the minimum active power is 0.242 p.u. and i^*_{Drd} and i^*_{Drq} are set as 0.79 and 0.76 p.u., respectively.

The active and reactive powers of the DFIG in Cases 1 and 2 are shown in Figs. 8*a* and *b*. In both conditions, the active power is about 0.18 p.u. The reactive power in Case 1 varies to 0.55 p.u. while 0.11 p.u. in Case 2. The power angles of the SG are shown in Fig. 8*c*. The amplitudes of the first three swings in Case 1 are 50.04°, 47.24° and 38.70°, respectively. Comparing to Case 2, the amplitudes of the first three swings in Case 2 decrease by 0.69°, 1.20° and 1.78°, which means with the reactive power of the DFIG increasing, the amplitude of the SG' power angle swinging decreases and the power angle stability becomes better.

The active and reactive powers of the DFIG in Cases 3 and 4 are shown in Figs. 9*a* and *b*. Without considering the overspeed protection of the DFIG, the reactive power of the DFIG in Case 3 (shown as the dashed line in Fig. 9*b*) is larger than that in Case 4. Thus, the amplitudes of the first three swings in Case 3 (shown as the dashed line in Fig. 9*d*) are smaller than those in Case 4 by 2.46°, 12.70° and 6.84°, respectively. The power angle stability of the SG in Case 3 is better than that in Case 4.

However, with considering the overspeed protection of the DFIG, the active power of the DFIG (shown as the dash-dotted line in Fig. 9*a*) is too small because of too large reactive power. The rotating speed of the DFIG generator exceeds the overspeed protection actuating value, 1.3 p.u., which leads to action of the overspeed protection and the DFIG shutdown. It has a great impact on the SG and results in the instability of the SG's power angle (shown as the dash-dotted line in Fig. 9*d*). In Case 4, with the LVRT control proposed, the maximum rotating speed of the DFIG generator reaches 1.25 p.u. and the overspeed protection is not activated. The DFIG keeps providing reactive power for the grid according to the controllable power range. The power angle of the SG reaches the maximum swinging amplitude 107.12° and stabilises at 42.30°. It avoids the instable situation in Case 3 which proves that the control method in Case 4 is able to improve the power angle stability of the SG effectively and keeps the rotating speed of the DFIG in a reasonable range.

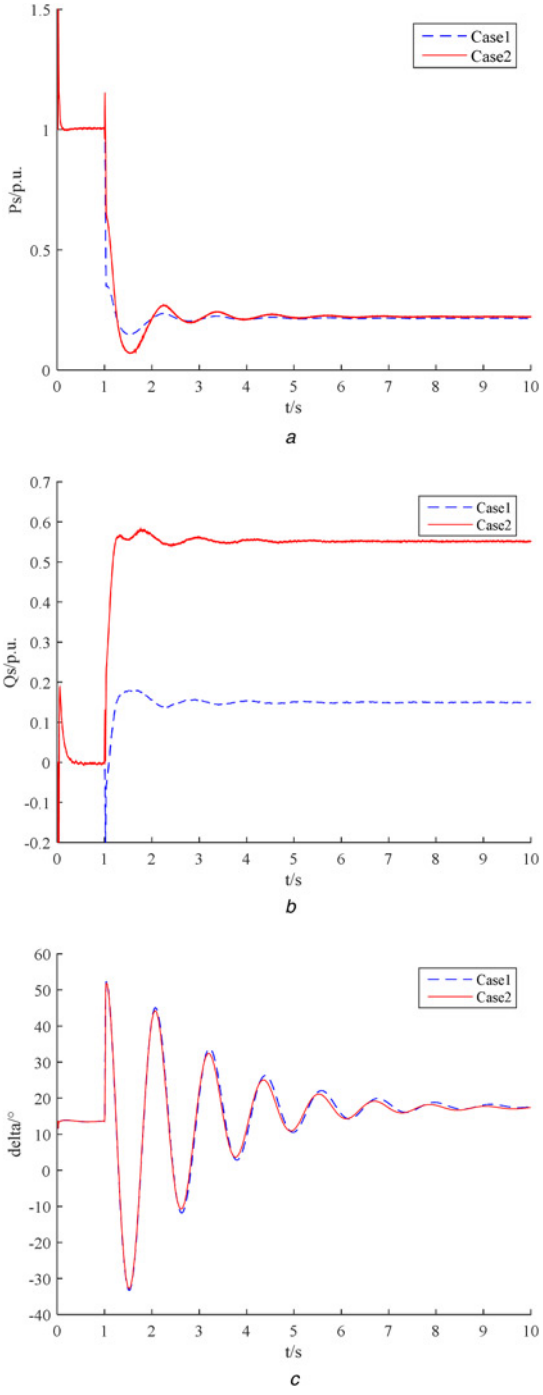

Fig. 8 *Simulation results of Cases 1 and 2*
a Active power of DFIG
b Reactive power of DFIG
c Power angle of SG

Table 1 Four conditions of simulation

No.	Wind speed, m/s	U_{DS}, p.u.	i^*_{Drd}, p.u.	i^*_{Drq}, p.u.
Case 1	15	0.7	0.4	0.3
Case 2			1	0.3
Case 3	15	0.28	1.08	0.20
Case 4			0.79	0.76

doi: 10.1049/joe.2017.0605

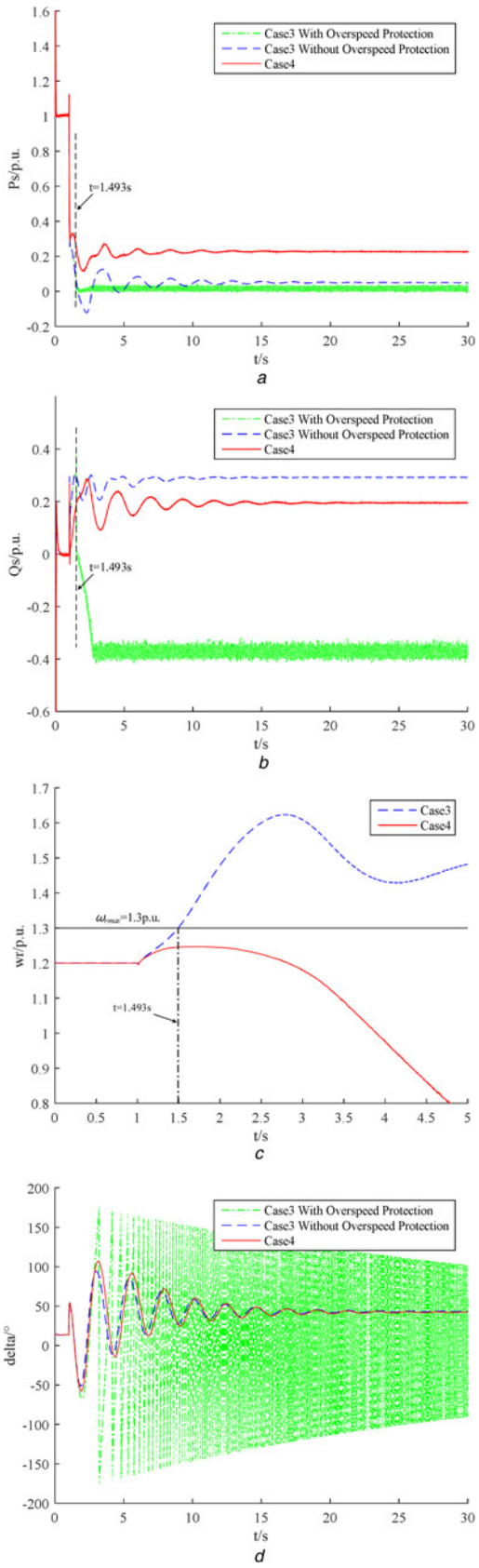

Fig. 9 *Simulation results of Cases 3 and 4*
a Active power of DFIG
b Reactive power of DFIG
c Rotor speed of DFIG
d Power angle of SG

6 Conclusions

The large number of DFIGs directly affects the power angle stability of the power system. Since controllable power range of the DFIG and the impact on the stability of the grid have not taken into consideration in current LVRT methods, the impact of the DFIG's short circuits current on the SG's stator voltage is analysed. The principle of the SG's transient stability varying with the influence of the DFIG is obtained. The controllable power range of the DFIG considering the speed limit is presented. Finally, an LVRT method of the DFIG for the SG's power angle stability improvement is proposed, which can make the best of transient controllable capacity of the DFIGURE. With this LVRT method, as the initial speed drops, the acceleration area for the DFIG generator's rotor is larger, which means smaller minimum active power, larger maximum reactive power and larger controllable power range. If the initial speed is smaller than a certain value, the minimum active power can be set as zero and the reactive power can achieve the maximum under the restriction of the RSC's current limit. This LVRT method can provide effective support for the power angle stability of the SG and benefit the formulation and implementation of the operation and control strategy of the power system containing large-scale wind power.

7 Acknowledgements

The authors were grateful for the support from the Natural Science Foundation of China (grant no. 51407017), the Smart Grid Technology and Equipment Key Special Foundation of National Key R&D Plan (grant nos. 2016YFB0900600 and 2017YFB0902005), the Chongqing Basic and Frontier Research Projects (grant no. cstc2015jcyjA90016).

8 References

[1] Junfeng L., '2014 China wind power review and outlook' (Chinese Renewable Energy Industries Assosiation, Beijing, 2014)
[2] State Grid Corp.: 'Technical rules for connecting wind farm to power system', in (Weisheng W, Yongning C, Huizhu D, *ET AL.* (eds.)): 'GB/T 19963-2011' (China Electric Power Press, Beijing, 2011)
[3] Edrah M., Lo K.L., Anaya-Lara O.: 'Impacts of high penetration of DFIG wind turbines on rotor angle stability of power systems', *IEEE Trans. Sustain. Energy*, 2015, **6**, pp. 759–766
[4] Muljadi E., Butterfield C.P., Parsons B., *ET AL.*: 'Effect of variable speed wind turbine generator on stability of a weak grid', *IEEE Trans. Energy Convers.*, 2007, **22**, pp. 29–36
[5] Lin L., Hou H., Li W., *ET AL.*: 'Simulation and comparison of transient stability of power system including DFIGs wind farm based on detailed model'. Int. Conf. Sustainable Power Generation and Supply, 2009. Supergen, 2009, pp. 1–6
[6] Hao Z.H., Yi-Xin Y.U.: 'The influence of doubly-fed induction generator on stability of power system', *Power Syst. Protect. Control*, 2011, **39**, pp. 7–14
[7] Tian X., Wang W., Chi Y., *ET AL.*: 'Performances of DFIG-based wind turbines during system fault and its impacts on transient stability of power systems', *Autom. Electr. Power Syst.*, 2015, **39**, pp. 16–21
[8] Yao J., Yu M., Chen Z., *ET AL.*: 'Coordinated control strategy for hybrid wind farms with DFIG and PMSG under symmetrical grid faults', *Trans. China Electrotech. Soc.*, 2017, **30**, pp. 26–36
[9] Engelhardt S., Erlich I., Feltes C., *ET AL.*: 'Reactive power capability of wind turbines based on doubly fed induction generators', *IEEE Trans. Energy Convers.*, 2011, **26**, pp. 364–372
[10] Lang Y.Q., Zhang X.G., Dian-Guo X.U., *ET AL.*: 'Reactive power analysis and control of doubly fed induction generator wind farm', *Proc. CSEE*, 2007, **27**, pp. 1–10
[11] Zhang Y., Yuan H.: 'Control strategy of DFIG main control system during low voltage ride through', *Electr. Power Autom. Equip.*, 2012, **32**, pp. 106–112
[12] Yu L., Qiang G., Xu C.: 'Improvement of low-voltage ride-through by coordinated pitch control and Crowbar control for DFIG wind turbine', *Electr. Power Autom. Equip.*, 2013, **33**, pp. 18–23

[13] Yin J., Bi T., Xue A., *ET AL.*: 'Study on short circuit current and fault analysis method of double fed induction generator with low voltage ride-through control strategy', *Cárnica*, 2015, **39**, pp. 60–62
[14] Kong X., Zhang Z., Yin X., *ET AL.*: 'Study of fault current characteristics of the DFIG considering dynamic response of the RSC', *IEEE Trans. Energy Convers.*, 2014, **29**, pp. 278–287
[15] Conroy J.F., Watson R.: 'Low-voltage ride-through of a full converter wind turbine with permanent magnet generator', *IET Renew. Power Gener.*, 2007, **1**, pp. 182–189
[16] Lopez J., Sanchis P., Roboam X., *ET AL.*: 'Dynamic behavior of the doubly fed induction generator during three-phase voltage dips', *IEEE Trans. Energy Convers.*, 2007, **22**, pp. 709–717

doi: 10.1049/joe.2017.0605